Energy Conversion and Management 146 (2017) 43–51

Contents lists available at ScienceDirect

Energy Conversion and Management

journal homepage: www.elsevier.com/locate/enconman

Performance analysis of hydrate-based refrigeration system

Wenxiang Zhang, Yanhong Wang, Xuemei Lang, Shuanshi Fan *

Key Lab of Enhanced Heat Transfer and Energy Conservation, Ministry of Education, School of Chemistry and Chemical Engineering, South China University of Technology, Guangzhou 510640, China

ARTICLE INFO

Article history:
Received 21 January 2017
Received in revised form 26 April 2017
Accepted 26 April 2017

Keywords:
Hydrate
Refrigeration
Coefficient of performance
Aspen Plus
Simulation

ABSTRACT

A novel refrigeration system called hydrate-based refrigeration system was proposed, and its performance was analyzed by using Aspen Plus. The system consisted of five parts, compressor/pump, hydrate formation tank, hydrate dissociation tank, expander and gas/liquid separator. Compared with conventional compression refrigeration cycle, hydrate-based refrigeration system uses hydrate formation tank to replace condenser to achieve heat release; hydrate dissociation tank for evaporator of achieve refrigeration. There were three types of the hydrate-based refrigeration system, which refrigeration cycles were analyzed through using Aspen Plus. Methyl fluoride, cyclopentane/monofluoro cyclopentane and water were used to form hydrate as the working fluids. For the system of methyl fluoride, cyclopentane and water, the highest coefficient of performance was 8.01–8.97, For the system of methyl fluoride, monofluoro cyclopentane and water, the best coefficient of performance was 7.58–8.49. Based on it, the relation of temperature and entropy during refrigeration process for hydrate-based refrigeration system was analyzed. It's coefficient of performance was 2–4 times of the conventional compression refrigeration.

1. Introduction

The economic growth and technology development of every country depended on the energy [1]. The available energy reflected the living quality [2]. With the energy crisis, the energy-efficient technology was extremely urgent. At present, heating, ventilation, and air-conditioning had consumed a large amount of energy [3]. Chinese total electricity consumption was 5.55 trillion kW h in 2015, rising 0.5% year-to-year, and the air conditioning accounted for above 30% of total electricity consumption [4]. Air conditioning system had a great energy-saving potential.

The main commercial air conditioning in society includes vapor compression refrigeration system, absorption refrigeration and ejector refrigeration currently. In air-conditioning system, energy-saving technology includes heat exchanger design [5], refrigerants selecting, and so on. There were three generations of refrigerants. The earliest refrigerants were ethyl ether, carbon dioxide, ammonia and sulfur dioxide. The second generation was Freon, such as CFCs, HCFCs, and HFCs. Sag and Ersoy [6] reported the COP of an ejector expansion refrigeration system of tetrafluoroethane (R134a) worked as refrigerants was 2.6–3.0. Liu et al. [7] reported the coefficient of performance (COP) of the refrigeration system of difluoromethane/hexafluoropropane (R32/R236fa) worked as refrigerants was 2.42–4.14. Jafari et al. [8] reported the COP of the refrigeration system of R134a worked as refrigerants was 2.6–4.1. The third generation was working pairs, such as lithium bride-water, lithium chloride-water, ammonia-water, whose COP was still low [9]. For the working pair of the lithium chloride-water, its' COP was just 0.589–0.891 [10]. And for the working pair of the ammonia-water, Singh et al. reported its' COP was just 0.707–0.776 [11], while Gogoi and Konwar reported its' COP was 0.697–0.877 [12]. The newest refrigerant was the materials of 0 ODP, low GWP. COP of the refrigeration system was improved little through the above methods. The cycle was the key of the improvement of the COP. There were few researches on the change of the cycle. And the COP of the new cycle of absorption refrigeration was low.

In recent years some researchers begun to utilize hydrate to change the cooling cycle. Hydrate was mainly applied on cool storage air conditionings design, flow performance, thermodynamic and capability of cold storage. Douzet et al. [13] designed a real size air-conditioning system using a tetrabutyl ammonium bromide (TBAB) semiclathrate hydrate slurry as secondary two-phase refrigerant. Delahaye et al. [14,15] studied the rheological properties of tetra-n-butyl phosphonium bromide (TBPB) and carbon dioxide (CO_2) worked as the cold storage media. Lin et al. [16] made research on the thermodynamic properties of semiclathrate

* Corresponding author.
E-mail address: ssfan@scut.edu.cn (S. Fan).

http://dx.doi.org/10.1016/j.enconman.2017.04.091
0196-8904/

Nomenclature

R41/CH_3F methyl fluoride
H_2O water
CP cyclopentane
FCP monofluoro cyclopentane
T temperature
p pressure
Q heat
COP coefficient of performance
c constant pressure specific heat of unit mass
S area of the cooling region
h height of the cooling region
ΔH enthalpy changes
G mass flow rate
M molecular mass
n molar quantity
w mass concentration
W power consumption
HBRS-A/B/C/D type A/B/C/D of HBRS
A/B/C/D type A/B/C/D of HBRS
S1/SA1/SB1/SC1 the heat of absorption
S2/SA2/SB2/SC2 energy consumption
1/A1/B1/C1 state 1
2/A2/B2/C2 state 2
3/A3/B3/C3 state 3
4/A4/B4/C4 state 4
5/A5/B5/C5 state 5
C6 state 6

Greeks symbols
ρ density
η proportion
α coefficient of heat dissipation

Subscripts
VCRS vapor compression refrigeration system
HBRS the hydrate-based refrigeration system
HBRS-A/B/C/D type A/B/C/D of HBRS
cc cooling capacity
a air
am ambient
in outlet air of the indoor conditioner
hydrate,n needed hydrate
diss dissociation
R41/CH_3F methyl fluoride
H_2O,n needed water
H_2O water
CP cyclopentane
FCP monofluoro cyclopentane
c gas compressor
p liquid pump
af air fan
s separator

hydrate, and Youssef et al. [17] studied the thermodynamic properties of CO_2 hydrate and TBPB semiclathrate hydrate. Zhang et al. [18] calculated the COP of cold storage by TBAB hydrate slurry was 1.95–2.50 for homogeneous storage, and 2.00–2.95 for heterogeneous storage. Hydrate refrigeration systems reduced the energy loss caused by cool supplied indirectly. Kim et al. [19] made the LCC analysis of CO_2 hydrate cooling system. Fournaison et al. [20,21] reported some gas hydrates have a high dissociation enthalpy around 500 kJ kg_{water}^{-1}, and addictives (such as sodium dodecyl sulfate) could significantly improve the flow properties of the slurry. The research found that COP of hydrate cool storage air conditioner was small, and it was not applicable for cooling at the high ambient temperature above 303 K.

Nowadays a novel hydrate refrigeration system was proposed [22]. Cool supply was achieved through hydrate dissociation at 278–298 K. Heat release was achieved by hydrate formation above 303 K. Ohmura et al. [23] found that R32, cyclopentane (CP) and TBAB mixture hydrate could form at 0.027–1.544 MPa and at temperatures from 280.4 K to 289.7 K, which meant CP can be used as efficient additive to moderate hydrate formation condition. Imai et al. [24] reported CP could moderate formation and dissociation condition of clathrate hydrate, which meant clathrate hydrate formation temperature achieved higher than 303 K under the pressure of lower than 5 MPa. Satoshi et al. [25,26] verified that the methyl fluoride (R41) and CP mixture hydrate can form at 293.7 K/305.9 K, 0.336 MPa/2.988 MPa. Hydrate can be used as hydrate-based refrigeration system (HBRS), which means R41 and CP or monofluoro cyclopentane (FCP) mixture can used as the working medium of hydrate refrigeration system. However, present HBRS can only achieve heat release at about 298 K, which COP is of 1–7. The COP is difficult to satisfy with the commercial demand under the condition of clean medium working as the refrigerants. At present work, based on the reported concept of hydrate refrigeration, the paper proposed a novel cycle of hydrate cooling. Gas and liquids in working fluids were pressurized and condensed separately to cut down the energy consumption of compressor. It replaced evaporation and condensation with hydrate formation and dissociation. During heat release, it compressed a little clean gas to reaction with water. It reduced compressor power consumption and achieved cool supply by hydrate dissociation after throttling expansion. So as to realize high performance of HBRS, the hydrate cool technologies, hydrate refrigeration process (the relation of temperature and entropy) and coefficient of performance were analyzed.

2. Hydrate-based refrigeration systems

HBRS Cool supply was achieved through hydrate dissociation at 278–282 K. Heat release was achieved by hydrate formation at 303 K. Ohmura et al. [23] found that the difluoromethane and cyclopentane mixture hydrate can form at 280.45–299.75 K and 0.027–1.544 MPa through thermodynamic model calculation and experimental test, which means difluoromethane and cyclopentane mixture can used as the working medium of hydrate refrigeration system. Imai et al. [24] reported the pair of difluoromethane and cyclopentane was one of the promising guest candidates suitable for a hydrate-based refrigerant. Mori et al. [22] verified hydrate could work as cool supply medium in the air conditioning system through gas and water reacting to form hydrate on high ambient temperature, 303–308 K. The hydrate-based refrigeration system achieved cool supply directly. In this paper, three kinds of the hydrate-based refrigeration system were proposed, HBRS-A is

multiphase compressor system, HBRS-B is single phase compressor with single phase pump (mixed cooling), and HBRS-C is single phase compressor with single phase pump (separated cooling).

2.1. Process design

Fig. 1 showed the flow sheet of HBRS-A. Hydrate dissociation tank worked as evaporator. Hydrate formation tank worked as condenser. Both of the gas and liquids were compressed by multiphase compressor. After multiphase compressor, mixture of pressurized gas and liquids flew into hydrate formation tank. Hydrate formed and heat was released to the environment. Then decompression, it flew into hydrate dissociation tank for refrigeration. Hydrate dissociation occurred in dissociation tank to absorb heat from cooling region and achieve refrigeration. And the cycle was achieved.

Fig. 2 showed the flow sheet of HBRS-B. Hydrate dissociation tank and hydrate formation tank also worked as evaporator and condenser respectively. Low pressure gas and liquids flew each own tubes. Gas compressor flew the gas and liquid pump flew the liquids separately. Pressurized gas and liquids mixed into the hydrate formation tank to form hydrate, heat release achieved. Formed hydrate flew into hydrate dissociation tank through decompression. Hydrate dissociated with heat absorption, and cooling was achieved. Gas and liquids after hydrate dissociation was separated through gas-liquid separator. Gas came into the gas compressor and water flew through pump. The system came into the next cycle.

HBRS-C was similar to HBRS-B, shown in Fig. 3. The difference was that gas and liquids released heat divided. Pressurized gas flowed into condenser to release the heat to the circumstance. Then it flowed into hydrate formation tank, mixed with liquids to form Hydrate.

2.2. System models

According to the process design of three types of HBRSs, HBRS-A, HBRS-B and HBRS-C, the paper set up the simulation flow sheet through Aspen Plus. Figs. 4, 5 and 6 showed the simulation models of HBRS-A, HBRS-B and HBRS-C respectively.

2.3. Working medium

Satoshi et al. [25,26] studied phase equilibrium on methyl fluoride (CH_3F/R41), cyclopentane (CP)/monofluoro cyclopentane (FCP) and water (H_2O). Experimental data was showed in Fig. 7. With the addictive of CP or FCP, it could moderate hydrate formation condition. Hydrate formation pressure was relatively lower under high temperature. In view of the experimental data, 4 points was selected, (305.9 K, 2.988 MPa) and (293.0 K, 0.336 MPa) for the system of R41, CP and H_2O, (306.2 K, 2.051 MPa) and (293.3 K, 0.206 MPa) for the system of R41, FCP and H_2O. It was selected as hydrate formation condition and dissociation condition of the HBRS performance simulation.

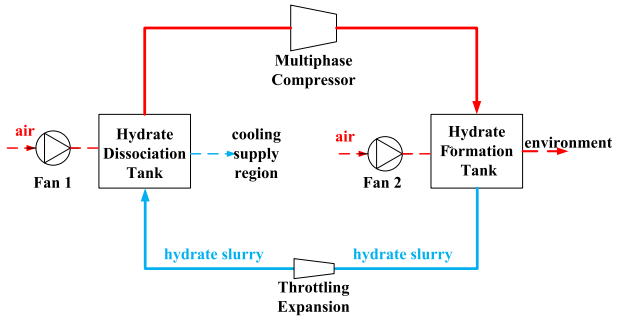

Fig. 1. Flow sheet of HBRS-A.

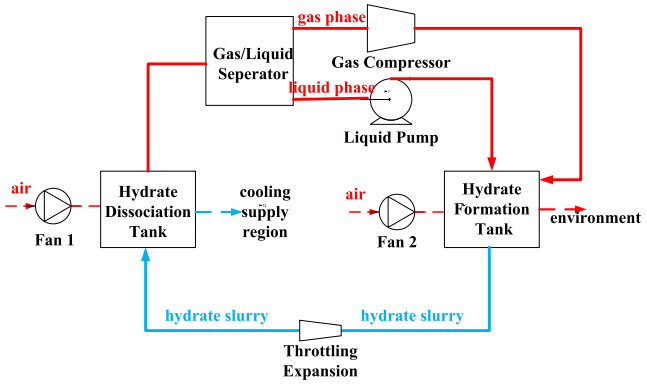

Fig. 2. Flow sheet of HBRS-B.

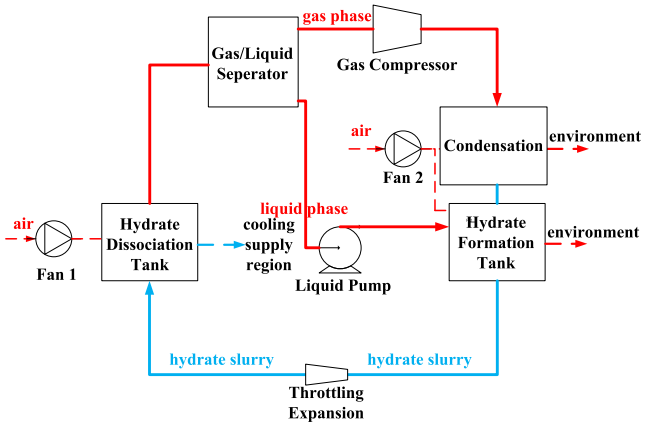

Fig. 3. Flow sheet of HBRS-C.

The dissociation enthalpy of hydrate was calculated through the Clapeyron equation. The dissociation enthalpy of R41 + CP + H_2O system under the condition of (305.9 K, 2.988 MPa) was 269.6 kJ/kg, while for R41 + FCP + H_2O system under the condition of (306.2 K, 2.051 MPa) was 247.2 kJ/kg. The dissociation enthalpy of this hydrate was higher than some other energy storage materials, such as organic phase change materials, inorganic phase change materials and eutectics [27]. And hydrate had a sufficient long term stability, while many phase change material had poor stability during thermal cycling [28].

Mass concentration of CP or FCP was set to be 50 wt%, and hydrate crystal presented type II. It was 16 small cages, 8 big cages and 136 water molecules. Big cages involved 28 water molecules, the rest formed small cages. The molecular structure of hydrate was $8C_5H_{10}{\cdot}28H_2O16CH_3F{\cdot}108H_2O$.

2.4. Simulation conditions

There was a trend for bedroom with study in settlement. Its area was around 20 m^2. In this paper, 20 m^2 were set to be refrigeration area. Ambient temperature was set to be 298–308 K. The outlet air temperature of the indoor unit of HBRS was set to be 287 K. Attain the capacity of cool supply through Eq. (1). Calculate the flow rate of refrigerant of the HBRS accordingly.

Attain total flow rate by energy conservation formula, refer to Eqs. (2)–(7). Flow rate of each substance could be attained. Proper-

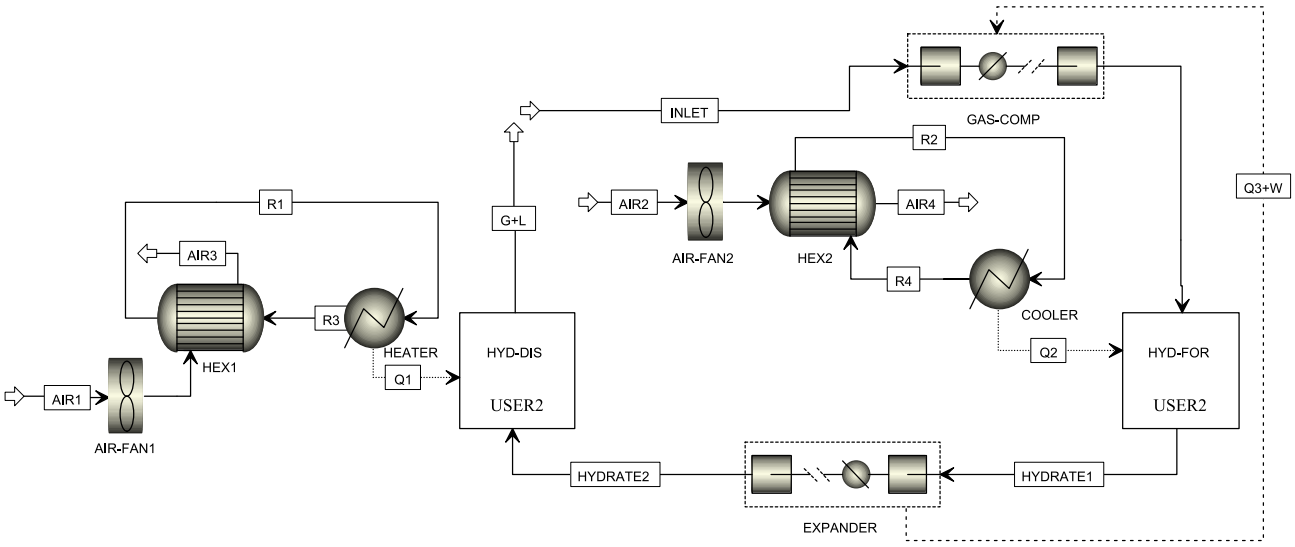

Fig. 4. Simulation model of HBRS-A.

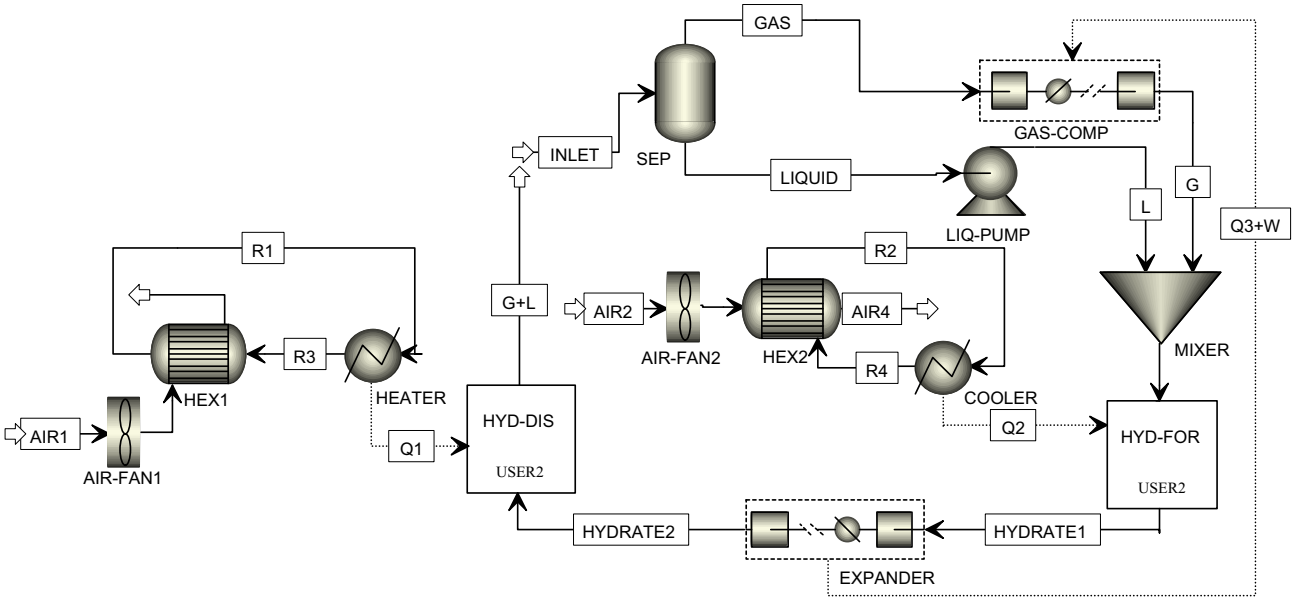

Fig. 5. Simulation model of HBRS-B.

ties of materials simulated by using Aspen Plus was shown in Table 1.

$$Q_{cc} = \frac{\alpha c_a \rho_a Sh(T_{am} - T_{in})}{3600} \quad (1)$$

$$G_{hydrate,n} = \frac{3600 Q_{cc}}{\Delta H_{diss}} \quad (2)$$

$$G_{R41} = \frac{G_{hydrate,n} M_{R41} n_{R41}}{M_{hydrate}} \quad (3)$$

$$G_{H_2O,n} = \frac{G_{hydrate,n} M_{H_2O} n_{H_2O}}{M_{hydrate}} \quad (4)$$

$$G_{H_2O} = G_{H_2O} + \frac{G_{hydrate,n}(1 - \eta_{H_2O})}{\eta_{hydrate}} \quad (5)$$

$$G_{CP} = G_{H_2O} w_{CP} \quad (6)$$

$$G_{FCP} = G_{H_2O} w_{FCP} \quad (7)$$

2.5. Coefficient of performance calculation

In general, the efficiency of any cooling system was measured by the coefficient of performance (COP), which was a measure of how efficiently the input energy was transformed to a useful output cooling effect [29]. It was defined as the ratio of cooling capacity to the energy supplied to the system [30]. In the HBRS, power-consuming units included the compressor, the pump, multiphase compressor and the air fan. COP of the HBRS was determined as Eqs. (8)–(10). For HBRS-A and HBRS-B, power consuming parts included gas compressor, liquid pump, air fan and separator. For HBRS-C, power consuming parts were consists of multiphase compressor and air fan. The paper used Aspen Plus to simulate cool

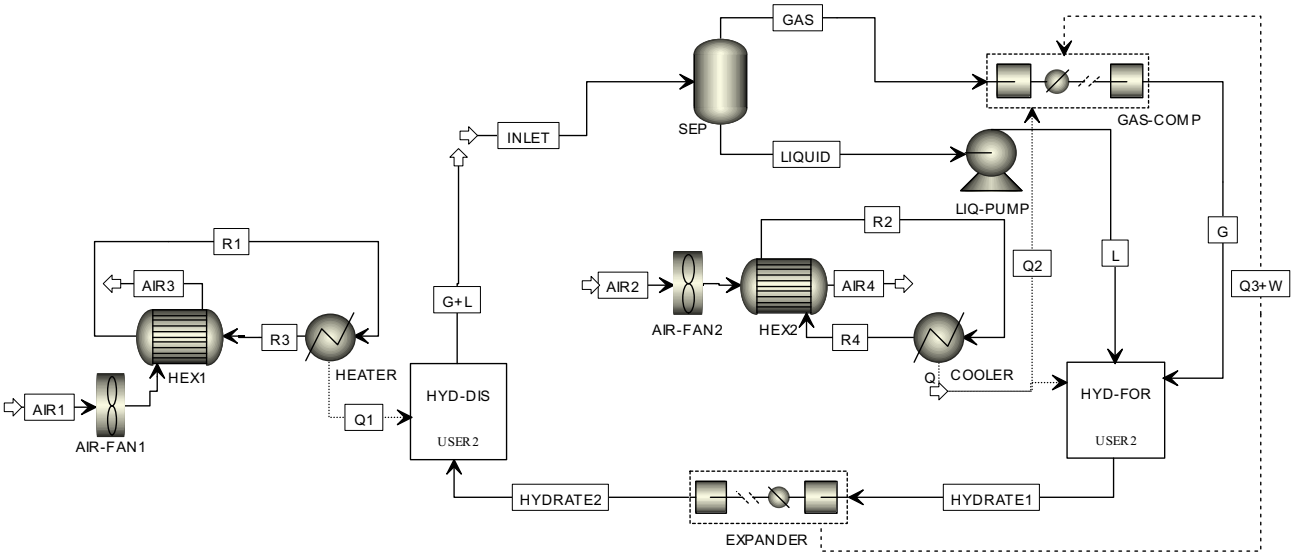

Fig. 6. Simulation model of HBRS-C.

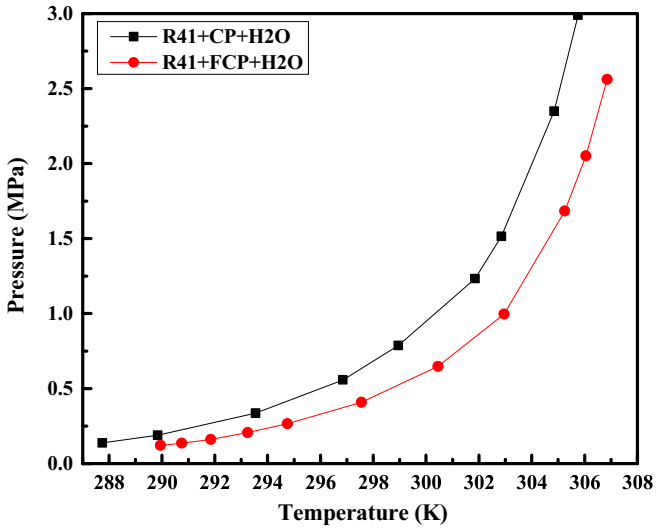

Fig. 7. Equilibrium p-T conditions for four phases involving clathrate hydrate formed with CH_3F (R41), CP/FCP and H_2O [25,26].

supply process in HBRS, and attained power consumption of each units. And then calculate the COP of different types of HBRS.

$$COP = \frac{Q_{cc}}{W} \tag{8}$$

$$COP = \frac{Q_{cc}}{W_c + W_p + W_{af} + W_s} \tag{9}$$

$$COP = \frac{Q_{cc}}{W_{mc} + W_{af}} \tag{10}$$

3. Results and discussion

The paper discussed the COP of the HBRS-A, HBRS-B and HBRS-C, which was up to 8. And this paper also analysis the changes of temperature and entropy (T-S) during the cooling process.

3.1. Coefficient of performance results

COP was the main index to reflect the capacity of refrigeration systems. The effect of temperature and unit on the COP of HBRSs was as follow.

3.1.1. Temperature factors

COP of different types of HBRS was changed with the ambient temperature. Table 2 showed the COP of the simulation of HBRS-A, B, C under the different temperatures with various refrigerants.

Table 1
Properties of materials simulated by Aspen Plus.

Temperature/K	R41 + CP + H_2O Flow rates/kg/h			R41 + FCP + H_2O Flow rates/kg/h		
	CH_3F/kg/h	CP/kg/h	H_2O/kg/h	CH_3F/kg/h	FCP/kg/h	H_2O/kg/h
298	3.47	17.64	35.28	3.72	19.02	38.03
299	3.79	19.25	38.49	4.05	20.75	41.49
300	4.10	20.85	41.70	4.48	22.74	45.48
301	4.42	22.45	44.91	4.82	24.49	48.98
302	4.74	24.06	48.11	5.16	26.24	52.47
303	5.05	25.66	51.32	5.51	27.99	55.97
304	5.37	27.26	54.53	5.85	29.74	59.47
305	5.68	28.87	57.74	6.20	31.48	62.97
306	6.00	30.47	60.94	6.54	33.23	66.47
307	6.31	32.08	64.15	6.89	34.98	69.96
308	6.63	33.68	67.36	7.23	36.73	73.46

Table 2
COP of the simulation under the different conditions.

Temperature/K	COP					
	R41 + CP + H_2O			R41 + FCP + H_2O		
	HBRS-A	HBRS-B	HBRS-C	HBRS-A	HBRS-B	HBRS-C
298	4.6	7.81	8.32	6.56	7.34	7.58
299	5.64	7.77	8.01	7.06	7.52	7.75
300	6.98	7.99	8.23	7.16	7.7	7.93
301	7.5	8	8.23	7.24	7.71	7.92
302	8.05	8.24	8.47	7.25	7.9	8.11
303	5.95	8.48	8.7	7.35	8.1	8.3
304	7.01	8.74	8.97	7.42	8.29	8.5
305	7.66	8.61	8.42	7.58	8.13	8.13
306	7.57	8.16	8.35	7.33	7.85	8.03
307	7.36	8.15	8.31	6.78	7.65	7.79
308	7.3	8.14	8.29	6.45	7.61	7.74

For HBRS-C in the system of R41, CP and H_2O, it showed the best performance, whose COP was up to 8.01–8.97, while 7.77–8.74 for HBRS-B and 4.60–8.05 for HBRS-A. In R41 + CP + H_2O system, the maximum value of COP of the HBRS-B and HBRS-C occurred under the condition of 304 K, while 302 K for HBRS-A, it was 8.74, 8.97 and 8.05 respectively. Since the temperature of hydrate formation was set to 305.8 K, the corresponding pressure of hydrate formation matches the set ambient temperature.

In the case of system of R41, FCP and H_2O, HBRS-C also showed the best performance, whose COP was 7.58–8.50, and the maximum of COP showed at 304 K. For HBRS-B, the COP was 7.34–8.29, and the maximum of COP also showed at 304 K. For HBRS-A, the COP was 6.45–7.58, and the maximum of COP also showed at 305 K.

HBRS showed the excellent performance of cooling. The coefficient of performance of all types remained a high level. Under the setting of the simulation, HBRS showed the best performance when the ambient temperature is close to the temperature of hydrate formation.

3.1.2. Unit factors

For in the system of R41, CP and H_2O, energy consumption distribution and the cooling capacity were shown in Fig. 8. Energy consumption equipments of HBRS-B and HBRS-C include air fan, gas compressor, liquid pump, gas/liquid separator. Energy consumption of gas/liquid separator, very close to zero, could be omitted here. HBRS-A includes air fan, multiphase compressor. The cooling capacity increases with the ambient temperature. Energy consumption of the gas compressor or multiphase compressor accounted for a large proportion of 54.5–62.2% in total consumption for HBRS-B while 53.3–64.2% for HBRS-C and 99.7–99.8% for HBRS-A. The proportion of the liquid pump was 34.4–38.8% for HBRS-B and 35.5–39.8% for HBRS-C. Air fan accounts for 2.1–7.3% for HBRS-B, 0.2–0.6% for HBRS-C, and 0.2–0.4% for HBRS-A.

For in the system of R41, FCP and H_2O, power consumption distribution and the cooling capacity were shown in Fig. 9. Similar to the above system, the cooling capacity increases with the ambient temperature. Energy consumption of the gas compressor or multiphase compressor accounts for the main content of 68.7–75.5% in total consumption for HBRS-B, 73.1–77.0% for HBRS-C and 99.6–99.8% for HBRS-A. The proportion of the liquid pump was 22.0–24.9% for HBRS-B and 22.7–25.5% for HBRS-C. Air fan accounted for 1.9–6.9% for HBRS-B, 0.2–0.4% for HBRS-C and HBRS-A.

Power consumption in the system went for flowing fluid. Gas compressor was used for flowing gas and compressing gas. Liquid pump was used for flowing water and compressing water. Air fan was used for flowing air indoor and outdoor. Multiphase compressor was used to press and flow the refrigerants which composed of

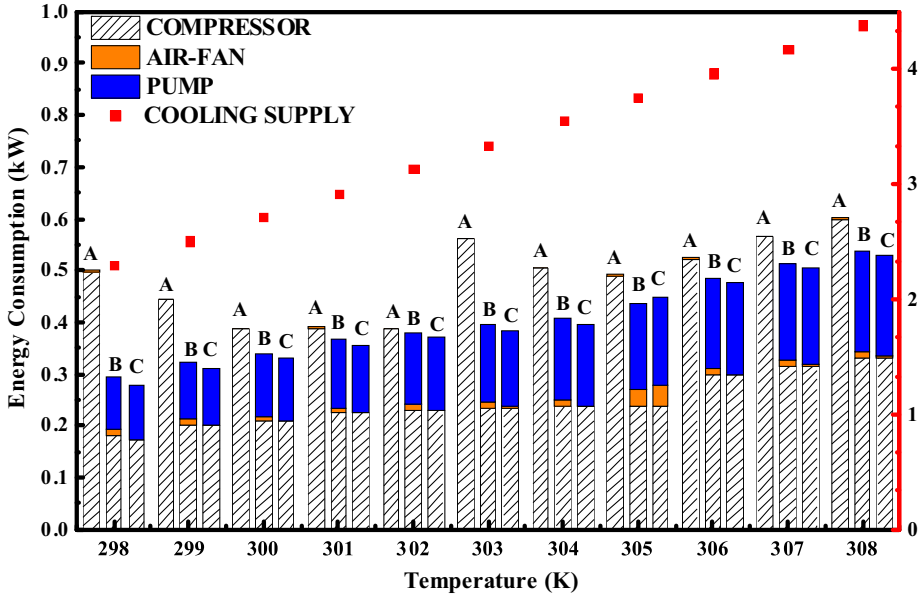

Fig. 8. Power consumption distribution and the cooling capacity in the system of R41, CP and H_2O.

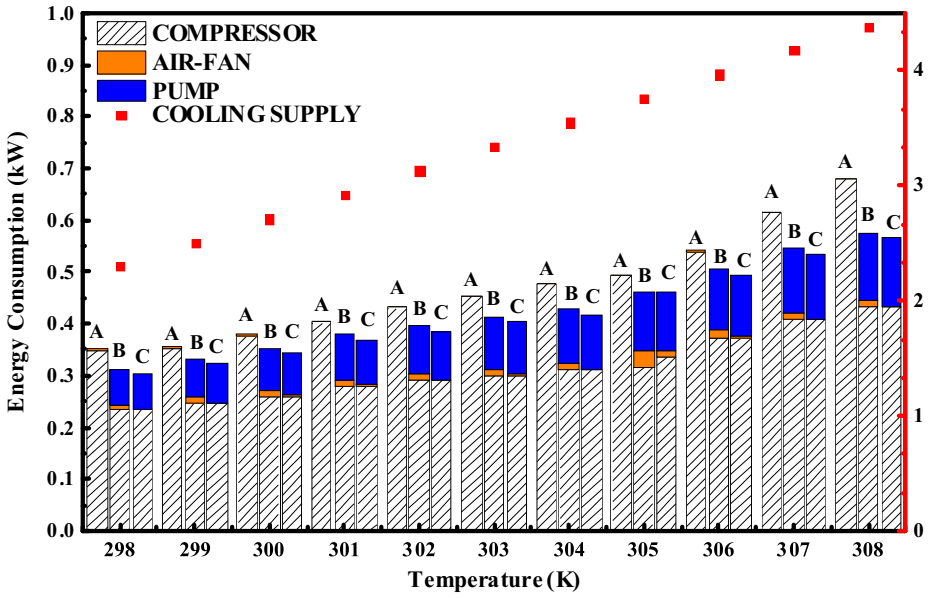

Fig. 9. Power consumption distribution and the cooling capacity in the system of R41, FCP and H_2O.

R41, CP/FCP and H_2O. The device which went for compressing fluids accounts for a very large proportion in total power consumption.

Since the compression ratio of the system of R41, CP with H_2O was 8.89 and the system of R41, FCP with H_2O was 9.96, the dissociation enthalpy of the hydrate for the different system was not the same. It results in the energy consumption for the system of R41, CP with H_2O was less than the other system of R41, FCP with H_2O.

3.2. Temperature and entropy diagram

In the HBRS-C system, evaporation and condensation were replaced with hydrate formation and dissociation. Gas and liquids formed hydrate to release heat and hydrate dissociated to gas and liquids to absorb heat, which supplied the cooling.

The relationship of temperature and entropy during cooling cycle was shown in Fig. 10. 1-2-3-4-5-1 meant the refrigeration process of vapor compression refrigeration system (VCRS). C1-C2-C3-C4-C5-C6-C1 meant HBRS-C cooling cycle. Both of the air

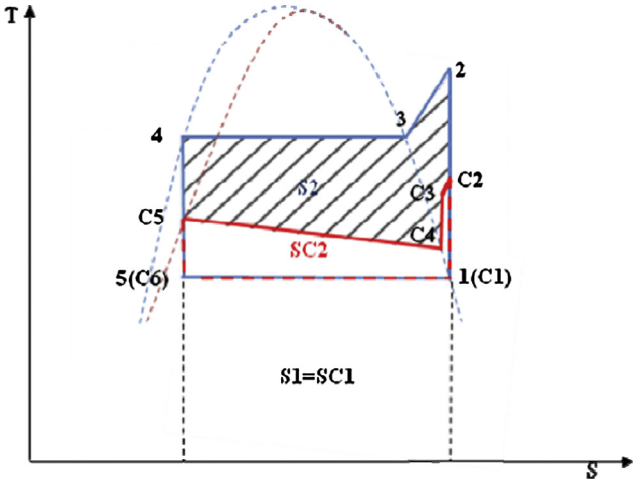

Fig. 10. T-S contrast of CCRC and HBRS-C.

conditioners included heat absorption, heat release, vapor compression and throttling expansion.

In VCRS, 1-2 meant adiabatic compression process. Refrigerant vapor with high temperature and high pressure was attained at the point 2. 2-3-4 meant condensation of gas vapor. Liquid refrigerant with high temperature and high pressure was attained at the point 4. 4-5 meant throttling expansion process, liquid with low temperature and low pressure was attained at the point 5. 5-1 meant evaporation. Liquid refrigerant was evaporated to the initial state at the point 1. Cooling supply was achieved. It was returned to state 1, and so on.

In HBRS-C, C1-C2 meant compression and pumping process. Refrigerant vapor with high temperature and high pressure was gotten at the point C2. C2-C3 meant air cooling process. The temperature of refrigerant vapor was reduced. C3-C4-C5 meant hydrate formation. Refrigerant vapor with high pressure and the liquid solution flowed into hydrate formation tank to form hydrate. C5-C6 meant expansion throttle. The temperature and pressure of hydrate became low enough for cooling. C6-C1 meant hydrate dissociation. Hydrate with low temperature and low pressure absorbed the heat of the cooling region to dissociate. Cooling supply was achieved. It was returned to state 1, and so on.

Air cooling of refrigerant vapor and hydrate formation heat replaced traditional condensation to release the heat to the atmosphere. Hydrate dissociation replaced traditional evaporation to absorb the heat from the cooling region. With the same refrigerating capacity, the heat absorption $Q_{VCRS} = Q_{HBRS-C} = S1 = SC1$. Energy consumption of the HBRS-C was W_{HBRS-C}, $W_{HBRS-C} = SC2$. Power consumption of VCRS was W_{VCRS}, $W_{VCRS} = S2$.

It was derived $COP_{HBRS-C} > COP_{VCRS}$. And $COP_{HBRS-C} = 2–4\ COP_{VCRS}$. HBRS-C consumed less power than VCRS. It possessed more energy-saving superiority.

For three types of HBRSs, temperature and entropy state of working fluids during cooling process were shown in Fig. 11. For the points A1, A2, A3, A4, and A5, it meant the cooling process of the HBRS-A. It consumed the most power among the three types of HBRSs. It was the earliest type of HBRS proposed by researches. A1-B1 meant compression. Mixture of refrigerant vapor and liquid solution with high pressure and high temperature was attained at the point A2. A2-A3-A4 meant air cooling and hydrate formation. Heat exchange efficiency was enhanced by the existing liquid solu-

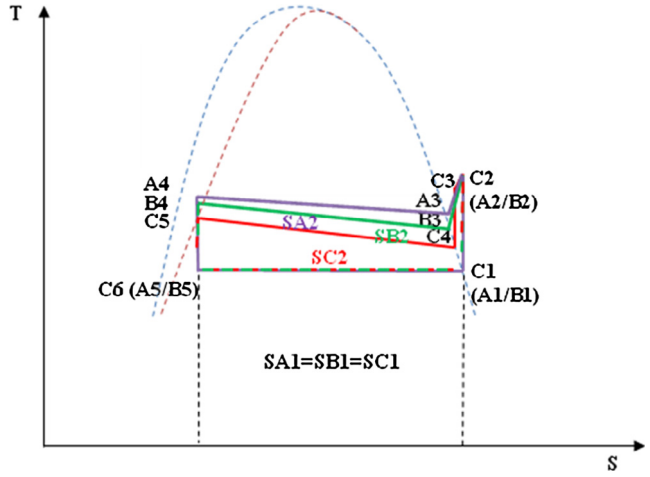

Fig. 11. T-S contrast of HBRS-A, HBRS-B and HBRS-C.

tion. Hydrate was attained at the point A4. A4-A5 meant expression throttle. Hydrate with low temperature and low pressure was attained at the point A5. A5-A1 meant hydrate dissociation, cooling supply was achieved, and so on.

Based on it, the paper presented to flow the refrigerant vapor and liquid solution separately which was HBRS-B. For points B1, B2, B3, B4, and B5, it meant the cooling process of the HBRS-B which was similar to HBRS-A. The difference was to use individual pressurization for refrigerant vapor and liquid solution. In the system, refrigerant vapor accounted for a relatively small proportion which made pressurization separately better. It resulted in low power consumption under the condition of compression separately. Therefore HBRS-B consume less power than HBRS-A.

The temperature change of gas was much more than liquids after compression. The paper proposed the third HBRS, which was HBRS-C. For points C1, C2, C3, C4, C5 and C6, it meant the cooling state point analysis of the HBRS-C. At the point C2, refrigerant vapor with high temperature was gotten. Condense the pressurized refrigerant vapor separately and turned to the point C3. Then refrigerant vapor and liquid solution mixed in the hydrate formation tank at the point C4. Hydrate was attained at the point C5. After expansion throttle and hydrate dissociation, it come to the point C1. It consumed the least power.

Hydrate was used to be the refrigerant in hydrate-based refrigeration systems which made full use of the sensible heat and the latent heat of vapor-liquid and liquid-solid. It made the hydrate-based refrigeration system expressed better cooling capacity than other cooling medium [27,28].

4. Conclusions

Air conditioning power consumption occupied a large proportion nowadays. A novel refrigeration system is proposed which called hydrate-based refrigeration system. HBRS, instead of evaporation and condensation of conventional air conditioner, cooled space through hydrate formation and dissociation. There are three types of hydrate-based refrigeration systems. HBRS-A is a multiphase compressor, HBRS-B is a single phase compressor with a single phase pump (mixed cooling), HBRS-C is a single phase compressor with a single phase pump (separated cooling). It is adopted methyl fluoride, cyclopentane, monofluoro cyclopentane and water to form hydrate as the refrigerant. Coefficient of performance is calculated.

The results show the highest coefficient of performance was 8.01–8.97, which is HBRS using methyl fluoride, monofluoro cyclopentane and water. Coefficient of performances of different types of hydrate-based refrigeration systems are changed with the ambient temperature. Analyzing temperature and entropy during refrigeration process for hydrate-based refrigeration systems find that coefficient of performance was three or four times of the conventional compression refrigeration. In hydrate-based refrigeration systems, the large proportion in total power consumption is used in compressing fluids, which hinders the improvement of the coefficient of performance of the hydrate-based refrigeration system. In future work, it is urgent to make hydrate dissociation pressure higher, cut pressure ratio down and find the materials whose value of dP/dT is smaller in the hydrate phase equilibrium curve. It can diminish power consumption in the hydrate-based refrigeration system and improve the coefficient of performance of the hydrate-based refrigeration system.

Acknowledgement

This work was supported by the National Natural Science Foundation of China (51576069), Guangdong Natural Science Foundation (2016A030313488).

Appendix A. Supplementary material

Supplementary data associated with this article can be found, in the online version, at http://dx.doi.org/10.1016/j.enconman.2017.04.091.

References

[1] Wang DC, Zhang JP, Yang QR, et al. Study of adsorption characteristics in silica gel–water adsorption refrigeration. Appl Energy 2014;113:734–41.
[2] Sarbu I, Sebarchievici C. Review of solar refrigeration and cooling systems. Energy Build 2013;67:286–97.
[3] Perez-Lombard L, Ortiz J, Pout C. A review on buildings energy consumption information. Energy Build 2008;40(3):394–8.
[4] The National Energy Administration of China released the total electricity consumption in 2015. The National Energy Administration of China; 2016. p. 1.
[5] Ge TS, Dai YJ, Wang RZ. Performance study of desiccant coated heat exchanger air conditioning system in winter. Energy Convers Manage 2016;123:559–68.
[6] Sag Nagihan Bilir, Ersoy H Kursad. Experimental investigation on motive nozzle throat diameter for an ejector expansion refrigeration system. Energy Convers Manage 2016;124:1–12.
[7] Liu Jian, She Xiaohui, Zhang Xiaosong. Experimental study of a novel double temperature chiller based on R32/R236fa. Energy Convers Manage 2016;124:618–26.
[8] Jafari Rahim, Okutucu-Özyurt Tuba, Ünver Hakkı Özgür, et al. Experimental investigation of surface roughness effects on the flow boiling of R134a in microchannels. Exp Therm Fluid Sci 2016;79:222–30.
[9] Jemaa Radhouane Ben, Mansouri Rami, Boukholda Ismail, et al. Experimental investigation and exergy analysis of a triple fluid vapor absorption refrigerator. Energy Convers Manage 2016;124:84–91.
[10] Bellos Evangelos, Tzivanidis Christos, Antonopoulos Kimon A. Exergetic and energetic comparison of LiCl-H_2O and LiBr-H_2O working pairs in a solar absorption cooling system. Energy Convers Manage 2016;123:453–61.
[11] Singh Omendra Kumar. Performance enhancement of combined cycle power plant using inlet air cooling by exhaust heat operated ammonia-water absorption refrigeration system. Appl Energy 2016;180:867–79.
[12] Gogoi TK, Konwar D. Exergy analysis of a H_2O–LiCl absorption refrigeration system with operating temperatures estimated through inverse analysis. Energy Convers Manage 2016;110:436–47.
[13] Douzet J, Kwaterski M, Lallemand A, et al. Prototyping of a real size air-conditioning system using a TBAB semiclathrate hydrate slurry as secondary two-phase refrigerant – experimental investigations and modeling. Int J Refrig 2013;36(6):1616–31.
[14] Clain Pascal, Delahaye Anthony, Fournaison Laurence, et al. Rheological properties of tetra-n-butyl phosphonium bromide hydrate slurry flow. Can J Chem Eng 2012;194:112–22.
[15] Jerbi Salem, Delahaye Anthony, Oignet Jeremy, et al. Rheological properties of CO_2 hydrate slurry produced in a stirred tank reactor and a secondary refrigeration loop. Int J Refrig 2013;36(4):1294–301.
[16] Lin Wei, Dalmazzonea Didier, Fürst Walter, et al. Thermodynamic properties of semiclathrate hydrates formed from the TBAB + TBPB +water and CO_2 + TBAB + TBPB +water systems. Fluid Phase Equilibr 2014;372:63–8.
[17] Youssef Z, Hanu L, Kappels T, et al. Experimental study of single CO_2 and mixed CO_2 + TBAB hydrate formation and dissociation in oil-in-water emulsion. Int J Refrig 2014;46:207–18.

[18] Shi XJ, Zhang P. Cold storage by tetra-n-butyl ammonium bromide clathrate hydrate slurry generated with different storage approaches at 40 wt% initial aqueous solution concentration. Int J Refrig 2014;42:77–89.
[19] Choi Jae Woo, Kim Shol, Kang Yong Tae. CO_2 hydrate cooling system and LCC analysis for energy transportation application. Appl Therm Eng 2015;91:11–8.
[20] Oigneta Jérémy, Delahayea Anthony, Torré Jean-Philippe, et al. Rheological study of CO_2 hydrate slurry in the presence of Sodium Dodecyl Sulfate in a secondary refrigeration loop. Chem Eng Sci 2017;158:294–303.
[21] Anthony Delahaye, Laurence Fournaison, Salem Jerbi, et al. Rheological properties of CO_2 hydrate slurry flow in the presence of additives. Ind Eng Chem Res 2011;50(13):8344–53.
[22] Ogawa T, Ito T, Watanabe KJ, et al. Development of a novel hydrate-based refrigeration system: a preliminary overview. Appl Therm Eng 2006;26:2157–67.
[23] Imai S, Okutani K, Ohmura R, et al. Phase equilibrium for clathrate hydrates formed with difluoromethane either cyclopentane or tetra-n-butylammonium bromide. J Chem Eng Data 2005;50:1783–6.
[24] Takeuchi F, Ohmura R, Yasuoka KJ. Statistical-thermodynamics modeling of clathrate-hydrate-forming systems suitable as working media of a hydrate-based refrigeration system. Int J Thermophys 2009;30:1838–52.
[25] Satoshi T, Keita Y, Ryo O. Phase equilibrium for structure II hydrates formed with methylfluoride coexisting with cyclopentane, fluorocyclopentane, cyclopentene, or tetrahydropyran. J Chem Eng Data 2008;53:531–4.
[26] Satoshi T, Ryo O. Phase equilibrium for structure I and structure H hydrates formed with methyl fluoride and methyl cyclohexane. J Chem Eng Data 2007;52:635–8.
[27] Sharma Atul, Tyagi VV, Chen CR, et al. Review on thermal energy storage with phase change materials and applications. Renew Sustain Energy Rev 2009;13:318–45.
[28] Zalba Belen, Marıın Jose M, Cabeza Luisa F, et al. Review on thermal energy storage with phase change: materials, heat transfer analysis and applications. Appl Therm Eng 2003;23:251–83.
[29] Hassan HZ, Mohamad AA. Thermodynamic analysis and theoretical study of a continuous operation solar-powered adsorption refrigeration system. Energy 2013;61:167–78.
[30] Jain Vaibhav, Sachdeva Gulshan, Kachhwaha SS. NLP model based thermo-economic optimization of vapor compression-absorption cascade refrigeration system. Energy Convers Manage 2015;93:49–62.